TẠP CHÍ ISSN: 1859-316X
KHOA HỌC CÔNG NGHỆ HÀNG HẢI
JOURNAL OF MARINE SCIENCE AND TECHNOLOGY

LARGE DEFLECTION OF FG-CNTRC SANDWICH BEAMS PARTIALLY RESTING ON A TWO-PARAMETER ELASTIC FOUNDATION

CHUYỂN VỊ LỚN CỦA DẦM SANDWICH FG-CNTRC NẰM MỘT PHẦN TRÊN NỀN ĐÀN HỒI HAI THAM SỐ

BUI THI THU HOAI[1,2*], TRAN THI THU HUONG[1], NGUYEN DINH KIEN[2]

[1]*Faculty of Vehicle and Energy Engineering, Phenikaa University, Yen Nghia, Ha Dong, Hanoi, Vietnam*

[2]*Graduate University of Science and Technology, VAST, 18 Hoang Quoc Viet, Hanoi, Vietnam*

**Email: hoai.buithithu@phenikaa-uni.edu.vn*

Abstract

Large deflections of FG-CNTRC sandwich beams partially supported by a two-parameter elastic foundation are studied in this paper by a nonlinear finite element procedure. The core of the beams is homogeneous while the top and bottom are of CNTRC material. The effective properties of the two CNTRC face sheets are determined by an extended rule of mixture. CNTs are reinforced into matrix phase through uniform distribution (UD) or four different types of functionally graded (FG) distribution named as FG-X, FG- FG-V, FG-O. Based on a total Lagrange formulation, a first-order shear deformable nonlinear beam element is formulated and employed in the study. Newton-Raphson iterative method is used in combination with arc-length control technique to obtain the large deflection curves of the beams. The effects of CNT volume fraction, type of CNT distributions, layer thickness ratio and the foundation parameter on the large deflection behavior of the sandwich beams are examined and discussed.

Keywords: *FG-CNTRC sandwich beam, elastic foundation, total Lagrange formulation, large deflection analysis.*

Tóm tắt

Bài báo nghiên cứu chuyển vị lớn của dầm sandwich làm từ vật liệu composite được gia cường bởi các ống nano carbon (functionally graded carbon nanotube-reinforced composite, FG-CNTRC) nằm một phần trên nền đàn hồi bằng cách sử dụng phương pháp phần tử hữu hạn. Dầm được tạo bởi ba lớp vật liệu, trong đó lớp lõi được làm từ vật liệu thuần nhất và hai lớp ngoài được làm từ vật liệu FG-CNTRC. Tính chất vật liệu của hai lớp CNTRC được xác định bởi quy luật phối trộn mở rộng. Các kiểu phân bố khác nhau của CNTs được sử dụng trong nghiên cứu này bao gồm phân bố đều (UD) và bốn kiểu phân bố theo quy tắc hàm (FG) đó là FG-X, FG- FG-V, FG-O. Dựa trên phương pháp Lagrange toàn phần, lý thuyết phần tử dầm phi tuyến biến dạng trượt bậc nhất được thiết lập và sử dụng. Phương pháp lặp Newton-Raphson được sử dụng kết hợp với kĩ thuật kiểm soát độ dài cung để thu được đường cong chuyển vị lớn của dầm. Ảnh hưởng của tỉ phần thể tích CNT, kiểu phân bố CNT, tỉ số chiều dày của các lớp và tham số nền đàn hồi đối với ứng xử chuyển vị lớn của dầm được minh họa và thảo luận chi tiết trong nghiên cứu này.

Từ khóa: *Dầm sandwich FG-CNTRC, nền đàn hồi, phương pháp Lagrange toàn phần, phân tích chuyển vị lớn.*

1. Introduction

Functionally graded (FG) sandwich structures with outstanding properties in the high strength-to-weight ratio are extensively used in different engineering applications, such as automotive, aerospace and defense. With the increment of using high performance material in practice, such as FG-CNTRC material [1,2], the structures can undergo large deformation before failure, and this phenomenon accelerates the importance of nonlinear analysis in the field of structural mechanics. Nguyen and Tran [3] presented a large displacement analysis of FGM sandwich beams and frames using a co-rotational Euler-Bernoulli beam element. Hoai et al. [4] studied the large displacements of FG functionally graded sandwich beams in thermal environment using a finite element formulation.

The present paper studies large deflections of the FG-CNTRC sandwich beams partially resting on a two-parameter elastic foundation by using a nonlinear finite element procedure. The core of the beams is homogeneous while the two face sheets are made from CNTRC material. CNTs are reinforced into matrix phase through five type distributions namely UD, FG-X, FG-Λ, FG-V, FG-O. Based on the total Lagrange formulation, a nonlinear element is derived and used to compute the deflections of the beams. The effects of the CNT volume fraction, type of CNT distribution, layer thickness ratio and aspect ratio on the large deflection response of the sandwich beams are examined and discussed.

2. FG-CNTRC sandwich beam

Figure 1 shows the sandwich beam partially supported by two-parameter elastic foundation. The beam consists of three layers, a homogeneous core and two FG-CNTRC face sheets. Denoting $h_0=-\frac{h}{2}, h_1, h_2, h_3=\frac{h}{2}$, respectively, are the coordinates along the z-axis of layers. Five types of distribution of CNTs in the beam cross-section (UD, FG-X, FG-Λ, FG-V, FG-O), are investigated in this present work.

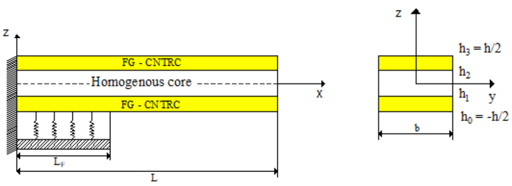

Figure1. Schematic view of an FG-CNTRC sandwich beam

The material properties of CNTRC layers are determined according to an extended rule of mixture as [1]:

$$E_{11}=\eta_1 V_{CNT} E_{11}^{CNT}+V_m E^m;$$
$$\frac{\eta_2}{E_{22}}=\frac{V_{CNT}}{E_{22}^{CNT}}+\frac{V_m}{E^m};\ \frac{\eta_3}{G_{12}}=\frac{V_{CNT}}{G_{12}^{CNT}}+\frac{V_m}{G^m} \tag{1}$$

in which, E_{11}^{CNT}, E_{22}^{CNT} and G_{12}^{CNT} are, respectively, Young's moduli and shear modulus of the CNT; E^m, G^m and $V_m=1-V_{CNT}$ are Young's modulus, shear modulus and volume fraction of matrix phase, respectively; η_1,η_2,η_3 are the CNT efficiency parameters. The Poisson's ratios of the FG-CNTRC face sheets are determined as:

$$\nu_{12}=V_{CNT}\nu_{12}^{CNT}+V_m\nu^m;\quad \nu_{21}=\frac{\nu_{12}}{E_{11}}E_{22}; \tag{2}$$

where ν_{12}^{CNT}, ν^m are Poisson's ratios of the CNT and matrix, respectively. The effective elastic and shear moduli of the kth layer are calculated as [1]:

$$E^{(k)}(z)=\frac{E_{11}}{1-\nu_{12}\nu_{21}};\ G^{(k)}(z)=G_{12}\ (k=1,3);$$
$$E^{(2)}=E^c;\ G^{(2)}=G^c \tag{3}$$

with E^c, G^c are the elastic and shear moduli of the core material. The effective mass density of the kth layer is defined as

$$\rho^{(k)}(z)=V_{CNT}\rho^{CNT}+V_m\rho^m\quad (k=1,3);$$
$$\rho^{(2)}=\rho^c \tag{4}$$

with ρ^c is mass density of core material.

3. Finite element formulation

Taking into account the variation of the material properties in the beam thickness, a two-node shear deformable beam element based on the Antman's nonlinear beam model [5] using the total Lagrange formulation is considered herewith

$$\mathbf{d}=\{u_1\ \ w_1\ \ \theta_1\ \ u_2\ \ w_2\ \ \theta_2\}^T \tag{5}$$

where $u_i, w_i, \theta_i, (i=1,2)$ are the axial, transverse displacements and rotation at node i, respectively.

The beam element with length l is initially straight and lies on the x-axis as depicted in a Cartesian coordinate system (x,z) in Figure 2. A point P with abscissa x and its associated cross section S in the initial configuration become point P' and section S' in the deformed configuration. The deformation of the point P can be defined through an angle $\theta(x)$ - the rotation of the cross section S, and the current position vector $\mathbf{r}_{,x}(x)$ of the point P', as [6]:

$$\mathbf{r}_{,x}(x)=\frac{d\mathbf{r}(x)}{dx}=[1+\varepsilon(x)]\mathbf{e}_1+\gamma(x)\mathbf{e}_2 \tag{6}$$

Where:

$$\mathbf{e}_1=\cos\theta\,\mathbf{i}+\sin\theta\,\mathbf{j},\ \ \mathbf{e}_2=-\sin\theta\,\mathbf{i}+\cos\theta\,\mathbf{j} \tag{7}$$

are, respectively, the unit vectors, orthogonal and parallel to the current section S'. The curvature of the

TẠP CHÍ ISSN: 1859-316X
KHOA HỌC CÔNG NGHỆ HÀNG HẢI
JOURNAL OF MARINE SCIENCE AND TECHNOLOGY

beam $\kappa(x)$ at the point *P'* is given by:

$$\kappa(x)=\frac{d\theta(x)}{dx} \tag{8}$$

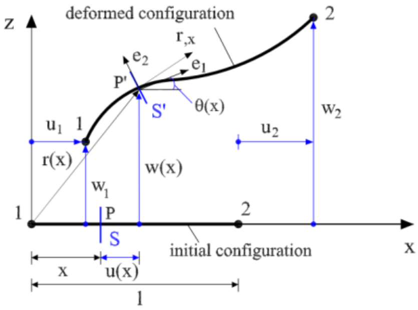

Figure 2. Configurations and kinematics of a two-node beam element

From Eqs. (6)-(8), one can write the axial and shear strains in the forms:

$$\begin{aligned}\varepsilon(x)&=\left(1+\frac{du}{dx}\right)\cos\theta+\frac{dw}{dx}\sin\theta-1,\\ \gamma(x)&=\frac{dw}{dx}\cos\theta-\left(1+\frac{du}{dx}\right)\sin\theta\end{aligned} \tag{9}$$

Noting that the strains $\varepsilon(x)$, $\gamma(x)$ and the curvature $\kappa(x)$ although parameterized for convenience by the reference abscissa $x\in[0,\ l]$ take the values on the current deformed configuration.

The strain energy for the beam element is given by:

$$U_B=\frac{1}{2}\int_0^l\left[\begin{aligned}&A_{11}\varepsilon^2(x)+2A_{12}\varepsilon(x)\kappa(x)\\&+A_{22}\kappa^2(x)+\psi A_{33}\gamma^2(x)\end{aligned}\right]dx \tag{10}$$

Where: $\psi=5/6$ is a shear correction factor; A_{11}, A_{12}, A_{22} and A_{33} are rigidities, defined as:

$$\begin{aligned}&(A_{11},A_{12},A_{22})=b\sum_{k=1}^{3}\int_{h_{k-1}}^{h_k}E^{(k)}(z)(1,\ z,\ z^2)dz;\\&A_{33}=b\sum_{k=1}^{3}\int_{h_{k-1}}^{h_k}G^{(k)}(z)dz\end{aligned} \tag{11}$$

The strain energy stored in the two-parameter elastic foundation resulting from the deformation of a beam element is given by:

$$\begin{aligned}U_F&=U_W+U_G\\&=\frac{k_W}{2}\int_0^l(u^2+w^2)dx+\frac{k_G}{2}\int_0^l(\theta-\gamma)^2dx\end{aligned} \tag{12}$$

where k_W and k_G are the stiffness of the Winkler foundation and the shear layer, respectively.

The displacements and rotation inside the element can be linearly interpolated from the nodal values according to:

$$\begin{aligned}&u=\frac{l-x}{l}u_1+\frac{x}{l}u_2,\ w=\frac{l-x}{l}w_1+\frac{x}{l}w_2,\\&\theta=\frac{l-x}{l}\theta_1+\frac{x}{l}\theta_2\end{aligned} \tag{13}$$

The above linear interpolation, however leads to an element with the shear-locking problem [4]. In order to deal with this problem, one-point Gauss quadrature is employed herewith to evaluate the strain energy of the element. In this regard, the strain energy of the beam element in the following form:

$$\begin{aligned}U&=U_B+U_F\\&=\frac{1}{2}l\left(A_{11}\bar{\varepsilon}^2+2A_{12}\overline{\varepsilon\kappa}+A_{22}\bar{\kappa}^2+\psi A_{33}\bar{\gamma}^2\right)\\&+\frac{l}{2}k_W\left(u^2+w^2\right)+\frac{l}{2}k_G\left(\bar{\theta}-\bar{\gamma}\right)^2\end{aligned} \tag{14}$$

Where:

$$\begin{cases}\bar{\varepsilon}=\left(1+\dfrac{u_2-u_1}{l}\right)\cos\bar{\theta}+\dfrac{w_2-w_1}{l}\sin\bar{\theta}-1\\ \bar{\gamma}=-\left(1+\dfrac{u_2-u_1}{l}\right)\sin\bar{\theta}+\dfrac{w_2-w_1}{l}\cos\bar{\theta}\\ \bar{\kappa}=\dfrac{w_2-w_1}{l};\ \bar{\theta}=\dfrac{\theta_1+\theta_2}{l}\end{cases} \tag{15}$$

The internal nodal force vector $\mathbf{f}_{in}$ and the tangent stiffness matrix $\mathbf{k}_t$ are computed by once and twice differentiating the strain energy with respect to the nodal displacement, respectively:

$$\mathbf{f}_{in}=\frac{\partial U}{\partial\mathbf{d}}=\mathbf{f}^{a}_{in}+\mathbf{f}^{c}_{in}+\mathbf{f}^{b}_{in}+\mathbf{f}^{s}_{in}+\mathbf{f}^{W}_{in}+ \tag{16}$$

$$\mathbf{k}_{in}=\frac{\partial^2U}{\partial\mathbf{d}^2}=\mathbf{k}^{a}_{t}+\mathbf{k}^{c}_{t}+\mathbf{k}^{b}_{t}+\mathbf{k}^{s}_{t}+\mathbf{k}^{W}_{t}+\mathbf{k}^{G}_{t} \tag{17}$$

where the superscrips a,c,b,s,W and G , respectively, indicate the terms contributed by the axial stretching, axial-bending coupling, bending, shear deformation of the beam, stretch of the Winkler foundation, and the rotation of the shear layer.

4. Equilibrium equation

The equilibrium equation for large deflection analysis of the beam can be written in the form [4]:

$$\mathbf{g}(\mathbf{p},\lambda)=\mathbf{q}_{\text{in}}(\mathbf{p})-\lambda\mathbf{f}_{ex}=\mathbf{0} \quad (18)$$

where the residual force vector $\mathbf{g}$ is a function of the current structural nodal displacements $\mathbf{p}$, and the load level parameter λ; $\mathbf{q}_{\text{in}}$ is the structural nodal force vector, assembled from the formulated vector $\mathbf{f}_{\text{in}}$; $\mathbf{f}_{\text{ex}}$ is the fixed external loading vector.

Eq. (18) can be solved by an incremental/iterative procedure. A convergence criterion based on Euclidean norm of the residual force vector is used for the iterative procedure as:

$$\| \mathbf{g} \| \leq \beta \| \lambda\mathbf{f}_{ex} \| \quad (19)$$

where β is the tolerance, chosen by 10^{-4} for all numerical examples considered in Section 5.

In order to handle the special cases where the tangent stiffness matrix ceases to be positive define, Newton-Raphson based iterative method is used herein in combination with spherical arc-length control technique in solving Eq. (18).

5. Numerical results

In this section, the following dimensionless parameters are introduced for the external loads and displacements:

$$P^*=\frac{E_s I}{L^2},\ u^*=\frac{u_L}{L},\ w^*=\frac{w_L}{L} \quad (20)$$

where I is the inertia moment of the cross section; u_L, w_L are the tip axial and vertical displacements, respectively.

As mentioned in the Introduction section, there are no available literatures related to large displacement analysis of FG-CNTRC sandwich beam, a homogenous beam subjected to a tip load P is analyzed herein to verify the formulation. The normalized tip displacements of the beam obtained herein compared to the available solution of Mattiasson [8] and Nanakorn and Vu [9] are given in Table 1. The good agreement between the displacements of the present work with that of Ref. [8] and Ref. [9] is seen from Table 1, regardless of the applied load.

Table 1. Comparison of tip response of homogenous beam under a tip load

P^*	$\|u^*\|$			w^*		
	Ref. [8]	Ref. [9]	Present	Ref. [8]	Ref. [9]	Present
3	0.25442	0.24757	0.25458	0.60325	0.59534	0.60434
5	0.38763	0.37733	0.38783	0.71379	0.70479	0.71541
7	0.47293	0.46103	0.47317	0.76737	0.75831	0.76950
9	0.53182	0.51909	0.53209	0.79906	0.79011	0.80169

Table 2. Tip response of FG-CNTRC sandwich beam under a tip load $P^*=15,\ L/h=20,\ \alpha=0.4$

(k_1, k_2)	Type	$h_c/h_f=4$			$h_c/h_f=6$			$h_c/h_f=8$		
		V^*_{CNT}			V^*_{CNT}			V^*_{CNT}		
		0.12	0.17	0.28	0.12	0.17	0.28	0.12	0.17	0.28
(50,0.5)	UD	0.9100	0.8967	0.8745	0.9085	0.8976	0.8789	0.9076	0.8983	0.8822
	FG-X	0.9098	0.8964	0.8742	0.9084	0.8975	0.8787	0.9075	0.8983	0.8821
	FG-O	0.9102	0.8969	0.8969	0.9086	0.8977	0.8790	0.9076	0.8984	0.8823
	FG-V	0.9063	0.8920	0.8681	0.9063	0.8947	0.8749	0.9061	0.8964	0.8795
	FG- Λ	0.8795	0.9016	0.8812	0.9107	0.9005	0.8829	0.909	0.9003	0.8849
(100,2.5)	UD	0.8765	0.8636	0.8426	0.8751	0.8646	0.8468	0.8743	0.8654	0.8500
	FG-X	0.8763	0.8634	0.8423	0.8751	0.8645	0.8467	0.8742	0.8653	0.8499
	FG-O	0.8767	0.8639	0.8429	0.8752	0.8647	0.8469	0.8743	0.8654	0.8501
	FG-V	0.8729	0.8591	0.8365	0.8730	0.8619	0.8430	0.8729	0.8635	0.8474
	FG- Λ	0.8803	0.8684	0.8489	0.8773	0.8674	0.8507	0.8757	0.8672	0.8526

TẠP CHÍ KHOA HỌC CÔNG NGHỆ HÀNG HẢI ISSN: 1859-316X
JOURNAL OF MARINE SCIENCE AND TECHNOLOGY

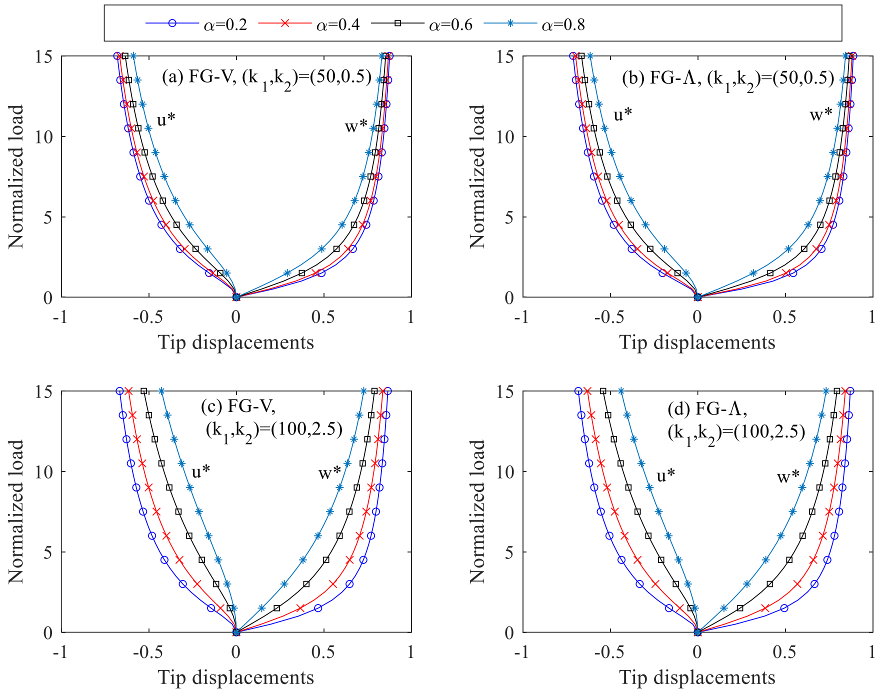

Figure 3. Load-displacement curves of FG-CNTRC sandwich beam under tip load

Table 2 presents tip response of FG-CNTRC sandwich beam under a tip load $P^*=15$ for five types of CNT distribution. The non-dimensional parameters $(k_1,k_2)=(50,0.5)$ and $(k_1,k_2)=(100,2.5)$ are computed respectively in this table. As can be seen that the tip response of the beam decreases with increasing of the total CNTs volume fraction V^*_{CNT}. Among the five type of CNT distribution, the FG-V leads to the smallest result, opposite to the FG-Λ, which gives the highest tip response, while the results obtained from three types UD, FG-X, FG-O are very close together. Table 2 also shows the effect of the ratio h_c/h_f on the tip response of the beam. The increase of the ratio h_c/h_f leads to the decrease in tip response of the beam. These results are resulted from the increase in the stiffness of the sandwich beam.

Figure 3 plots the load-displacement curves of FG-CNTRC sandwich beam under the tip load for difference values of foundation parameter α. At the given value of normalizied load, the tip displacements increase with the increasing of α.

6. Conclusions

The paper has investigated the large deflections of FG-CNTRC sandwich beam partially resting on two-parameter elastic foundation with five different types of CNT distribution for the first time. The obtained numerical results show that the CNT volume fraction, the type of CNT distributions and the foundation support play a vital role in the large deflection behavior of the sandwich beams. The formulation derived in the present work can be extended to count for the influence of other factors such as the temperature and porosities as well.

Acknowledgement

PhD. Student Bui Thi Thu Hoai was funded by Vingroup Joint Stock Company and supported by the Domestic Ph.D. Scholarship Programme of Vingroup Innovation Foundation (VINIF), Vingroup Big Data Institute (VINBIGDATA), code VINIF.2020.TS.15.

REFERENCES

[1] H. Wu and S. Kitipornchai. Free vibration and buckling analysis of sandwich beams with functionally graded carbon nanotube-reinforced composite face sheets, *International journal of structural stability and dynamics*, Vol.15, (7), 1540011, 2015.
DOI: 10.1142/S0219455415400118.

[2] F. Ebrahimi and N. Farazmand Nia. Thermo-mechanical vibration analysis of sandwich beams with functionally graded carbon nanotube-reinforced composite face sheets based on a higher-order shear deformation beam theory, *Mechanics of Advanced Materials and Structures*, Vol.24, 2017.
DOI: 10.1080/15376494.2016.1196786.

[3] D. K. Nguyen and T.T. Tran. A co-rotational formulation for large displacement analysis of functionally graded sandwich beam and frame structures, *Mathematical Problems in Engineering*, 2016.
http://dx.doi.org/10.1155/2016/5698351.

[4] B. T. T. Hoai, D. K. Nguyen, T. T. T. Huong and L. T. N. Anh. Large dispalcements of FGSW beams in thermal environment using a finite element formulation, *Vietnam Journal of Mechanics*, Vol. 42, pp.43-61. 2020.
DOI: https://doi.org/10.15625/0866-7136/14628

[5] S. S. Antman. *Nonlinear problems of elasticity*. Springer-Verlag, New York, 1995.

[6] C. Pacoste and A. Eriksson. Beam elements in instability problems. *Comput. Methods Appl. Mech. Eng*. Vol.144, pp.163-197. 1997.

[7] Y. Han and J. Elliott. Molecular dynamics simulations of the elastic properties of polymer/carbon nanotube composites, *Computational Materials Science*, Vol.39,(2), pp.315-323. 2007.

[8] K. Mattiasson. Numerical results from large deflection beam and fram problems analysed by means of elliptic intergrals, *Short Communication*, pp.145- 153. 1981.

[9] P. Nanakorn and L.N. Vu. A 2D field-consistent beam element for large displacement analysis using the total Lagrangian formulation, *Finite Elements in Analysis and Design*, Vol.42,,pp.1240-1247. 2006.

Received:	23 June 2021
Revised:	10 August 2021
Accepted:	18 August 2021